*31st EPS Conference on Plasma Phys. London, 28 June - 2 July 2004 ECA Vol.**28G**, P-5.108 (2004)*

Density Increase during Steady-state Plasma Discharge on the LargeHelical Device

R.Kumazawa[1], S.Sakakibara[1], K.Saito[1], T.Mutoh[1], T.Seki[1], T.Watari[1], Y.Nakamura[1], M.Sakamoto[2], T.Watanabe[1], N.Takeuchi[3], Y.Torii[4], F.Shimpo[1], G.Nomura[1], M.Yokota[1], A.Kato[1], H.Okada[4], Y.Zao[5] and LHD Experimental Group

[1]*National Institute for Fusion Science, Toki 509-5292, Japan*
[2]*Kyusyu University, Research Institute for Applied Mechanics, Kasuga, 816-8580, Japan*
[3]*Nagoya University, Faculty of Engineering, Nagoya 464-8601, Japan*
[4]*Kyoto University, Institute of Advanced Energy, Uji, 611-0011, Japan*
[5]*Academia Sinica Plasma Physics Institute, Hefei, 230031, People's Republic of China*

The long pulse plasma discharge with 150sec operation was achieved in the minority heating method of an ion cyclotron range of frequency (ICRF) heating on the Large Helical Device (LHD). The plasma of n_e=0.5~1.0x$10^{19}m^{-3}$ and $T_{e0}=T_{i0}$=1.5~2.0keV was sustained with the ICRF heating power of P_{RF}=0.5MW. However the electron density was gradually increased after the half discharge duration from n_e=0.5x$10^{19}m^{-3}$ to 1.0x$10^{19}m^{-3}$ at the end of the discharge. The observed electron density increase was closely related with a local increase in Hα intensity near the location of the ICRF heating antenna in the toroidal direction. The maximum temperature in the divertor plates was observed to be 400°C and is explained by calculating orbits of high-energy ions accelerated at the ion cyclotron resonance in front of the ICRF heating antenna.

1. Introduction

The ion cyclotron range of frequency (ICRF) heating was successfully carried out on the LHD employing the inward-shifted magnetic axis as well as installing the divertor plates [1~3]. It is experimentally proved that the optimized heating mode is obtained when the ion cyclotron resonance layer is located at the saddle point of the mod B surface. In this heating mode, minority ions absorb most of the injected RF power to form a high-energy ion tail and its energy is efficiently transferred to the bulk plasma [4]. A trial of a long pulse plasma discharge using an ICRF heated plasma was started in 1999. A long discharge of 68sec was achieved in the plasma with n_e=1.0x$10^{19}m^{-3}$ and the electron temperature on the axis T_{e0}=2.0keV with P_{RF}=0.7MW [5, 6]. The pulse length was limited by the RF generator problem. Then it was gradually prolonged from 68sec to 127sec in 2001 [7, 8]. The plasma duration time was seemed to be limited to the electron density increase up to the critical density depending the heating power; however data were not enough to analyze the cause of the density increase.

In this paper a long pulse plasma discharge sustained by ICRF heating only is reported. In Sec.2 the typical plasma discharge of the long pulse operation is described. Reasons limiting the plasma duration are analyzed. Then experimental data are compared with results obtained from an orbit calculation of high-energy ions accelerated at the ion cyclotron resonance layer. Then we summarize.

2. Experimental results

Time evolutions of plasma parameters of the long pulse plasma discharge are plotted in

Fig.1(a); this is the longest plasma discharge so far achieved in the ICRF heated plasma. The plasma with the electron density n_e=5~6x$10^{18}m^{-3}$, and the electron temperature and the ion temperature on the magnetic axis T_{e0}=T_{i0}=2.0keV was sustained with the ICRF heating power of P_{RF}=0.5MW. After 90 seconds the electron density was observed to be increase with the time accompanied an increase in the radiated power (P_{rad}) and to end up to n_e=1x$10^{19}m^{-3}$ with P_{rad}=250kW before the plasma suddenly disappeared at 150 seconds. The power supply from the RF generator was automatically ceased monitoring an increased reflected-power due to shrinking the plasma radius, when the plasma was collapsed. Besides several plasma parameters time evolutions of the vacuum pressure, the visible emission of Hα and HeI normalized by the electron density, and the temperatures increase in the divertor plates and in the vacuum wall are plotted in Fig.1(b): The vacuum pressure is increased by 3x10^{-5}Pa from P_V=2x10^{-4}Pa after 90s. The intensity of Hα signal (3-O vacuum port, which is near the ICRF heating antenna) was doubled. The temperature of the divertor plate (3-I, 3rd inboard section) was increased to 400^{o}C; as the time constant of the divertor plate is an order of 100s, the measured temperature is almost saturated. On the other hand the vacuum vessel temperature was increased by 3^{o}C; however as the time constant of the vacuum vessel is about 1 hour, the temperature increase was found to be small.

An electron density limit of the ICRF heated plasma was examined in the series of the experiments as shown in Fig.2. Experimental data are plotted in P_{ICH}(MW)-n_e($10^{19}m^{-3}$) plane. The critical electron density n_{ecr} at the heating power range of 0.2MW< P_{ICH} <1.5MW is given in the following relation; $n_{ecr}(10^{19}m^{-3}) = 1.8P_{RF}(MW)$. When the electron density is increased up to n_{ecr}, a radiated power fraction P_{rad}/P_{RF} is proportionally increased with a ratio of n_e/n_{ecr}, which is plotted by open circles in Fig.3. When the electron density was increased to n_e=1x$10^{19}m^{-3}$ at 150s as shown in Fig.1(a), P_{rad}/P_{RF} reaches 50% and then the plasma was terminated. In Fig.3 the behavior of P_{rad}/P_{RF} of this long pulse discharge is depicted against the normalized electron density n_e/n_{ecr}.

A toroidal asymmetry in Hα intensity [9] is plotted with open circles in Fig.4. This is an increased ratio, which is the value at t=150sec normalized by that at t=90sec. It is easily found that the increase in Hα is prominent in 3-O and is about 2.5 times larger than that in 8-O. The ICRF heating antennas are installed at 3.5, that is between 3-O and 4-O. This increase in the Hα intensity is assumed to be attributed to the temperature increase in the graphite plates located near 3-O in the toroidal direction. A toroidal asymmetry in the temperature increase in the inboard side divertor plate is also shown in Fig.4. It is found that the temperature increase in the 3-I (No.3 of inboard side divertor plate) is prominent. The 3-I divertor plate of 400^{o}C is thought to be a candidate of a hydrogen out-gassing source. This local temperature increase is compared with a calculation result of a particle orbit analysis. Two cyclotron resonance layers are separately located on the mod B surface in the employed magnetic configuration. The behavior of high-energy ions started at the cyclotron resonance layer (CRI) was examined using a full orbit calculation code [10, 11] under the RF electric field strength of 20kV/m [12]. About two thousands of high-energy ions with a

low initial energy were started from the upper (referred to as UICR) and the lower (referred to as LICR) ion cyclotron resonance layers in various initial phase difference against the RF electric field. The starting position was selected in 100 positions from R=4.15m to =4.20m (the last magnetic closed surface is at R=4.14m) along the ion cyclotron layer. Some of them hit the divertor plates within one circulation along the toroidal direction. The toroidal distribution of loss energy of high-energy ions is plotted in Fig.5 to compare the measured temperature increase as shown in Fig.4. This orbit calculation suggests that the local temperature increase in divertor plates can be mitigated in two ICRF heating scenarios, in which the ion cyclotron resonance is located on the magnetic axis in the minority heating or is located near the low magnetic field region in the mode conversion heating; there exists no ion cyclotron resonance layer in front of the ICRF heating antennas.

3. Summary

The long pulse plasma with 150sec operation was achieved on the LHD. The plasma of n_e=0.5~1.0x$10^{19}m^{-3}$ and T_{e0}=T_{i0}=1.5~2.0keV was produced with the ICRF heating power of P_{ICH}=0.5MW. More than 70MJ of the heating energy was injected. However the density increase limited the plasma pulse length. The local temperature increase in the divertor plates is thought to be a cause of the increase in the electron density. It can be understood counting loss energy of high-energy ions accelerated at the ion cyclotron resonance layers on the outer board side of the torus in front of ICRF heating antennas in the orbit calculation.

Acknowledgement

The authors would like to thank the scientists and the technical staff at the National Institute for Fusion Science who enables us to conduct these experiments.

References

[1] Saito K et al Nucl. Fusion **41** 1021

[2] Mutoh T et al Phys. Rev. Lett. **85** 4530

[3] Kumazawa R et al Phys. Plasmas **8** 2139

[4] Kumazawa et al., Plasma Phys. Controlled Fusion **43** 1191

[5] Kumazawa R, et al., J. Plasma and Fusion Research SERIES, Vol. 3 352

[6] Watari T et al., Nucl. Fusion **41** 325

[7] Seki et al., Proc. 14th Top. Conf. on RF power in Plasmas 595(2001) 334

[8] Mutoh T et al., Nucl. Fusion **43** 738

[9] Goto M., et al., Physics of Plasmas **5** 1402

[10] Matsumoto Y et al., Japanese Journal of Applied Physics 43 (2004) 332

[11] Watanabe T, et.al., to be published in 20th IAEA paper

[12] Saito K et al., to be published in J. Nucl. Mater.

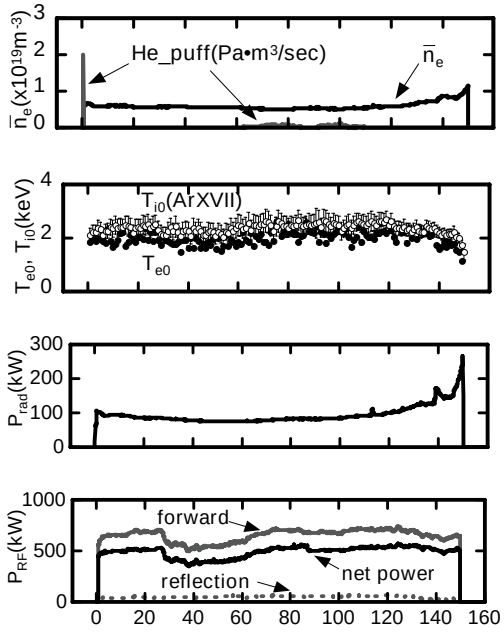

Fig.1(a) Time evolutions of plasma parameters, the electron density n_e, the electron T_{e0} and the ion temperature T_{i0} on the magnetic axis and the radiated power P_{rad} with the He gas puffing rate and the ICRF heating power P_{RF}.

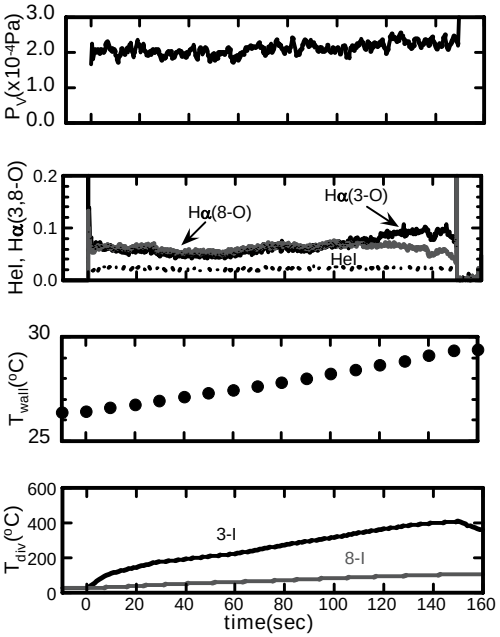

Fig.1(b) Time evolutions of the vacuum pressure P_V, the visible light emission of Hα and HeI, the temperature increase at the vacuum wall and at the divertor plates.

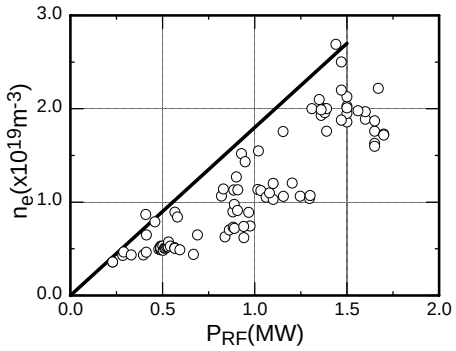

Fig.2 The relation between the critical electron density and the ICRF heating power.

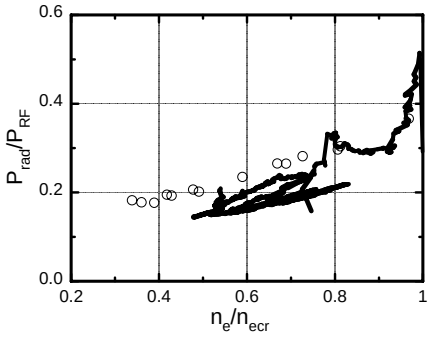

Fig.3 The fraction of the radiated power to the ICRF heating power vs. the ratio of the electron density to the critical electron density.

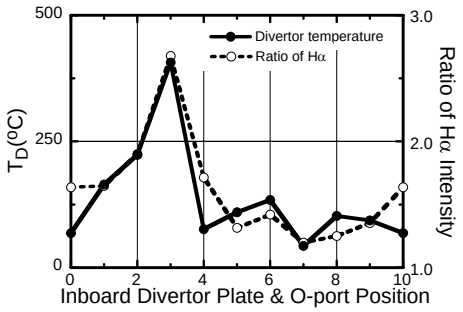

Fig.4 Toroidal distribution of temperature of the inboard divertor plates and ratio of Hα.

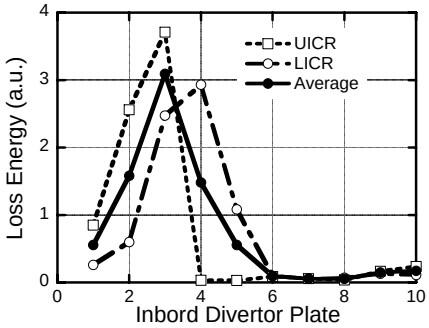

Fig.5 Toroidal distribution of loss energy of high-energy ions to divertor plates.